

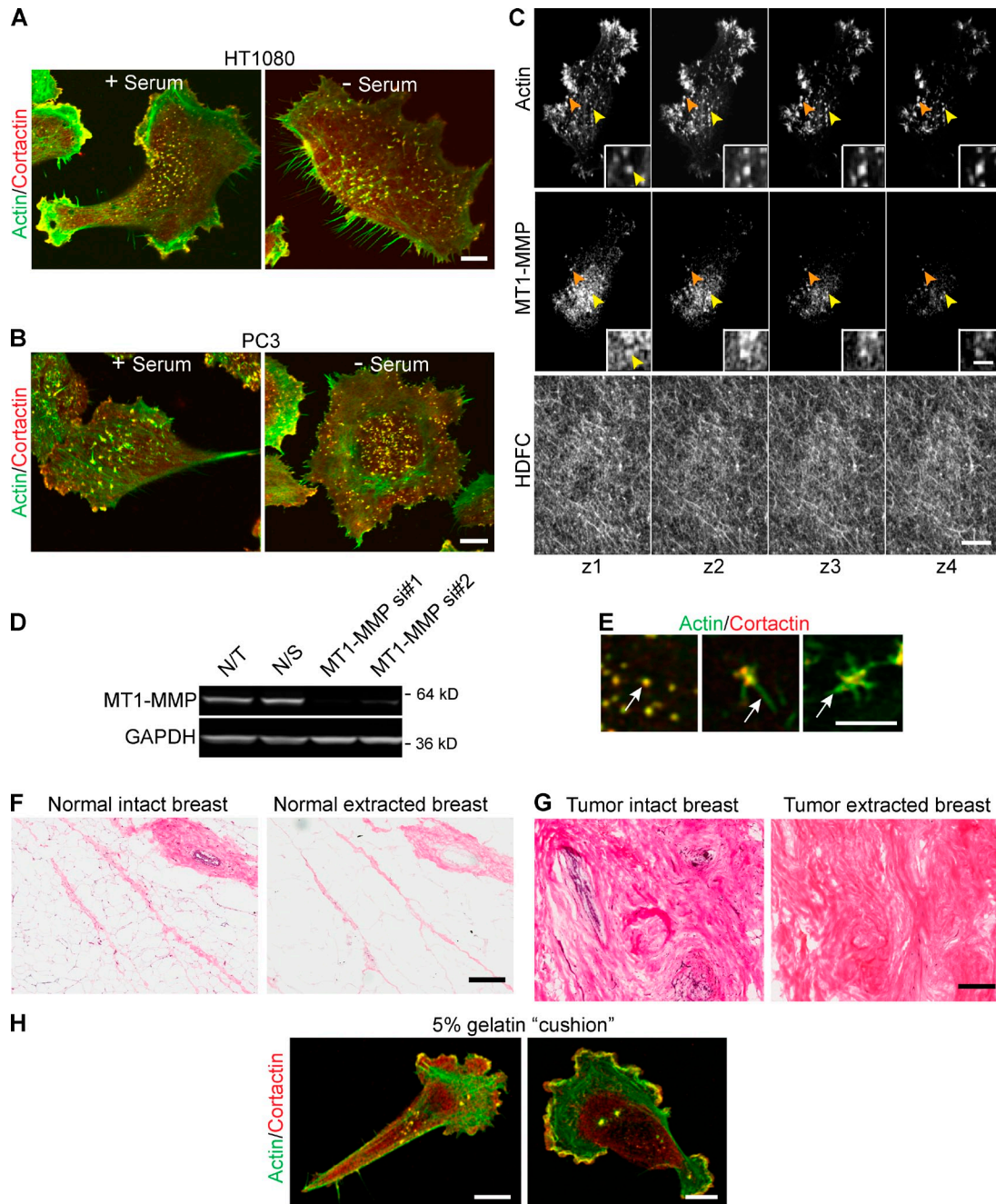
Artym et al., <http://www.jcb.org/cgi/content/full/jcb.201405099/DC1>

Figure S1. **HDFC is a potent inducer of invadopodia.** (A) HDFC induces abundant invadopodia in HT-1080 cells regardless of the presence or absence of serum in culture media. (B) HDFC induces abundant invadopodia in PC3 cells independent of serum. (C) Consecutive confocal z planes of MDA-MB-231 cells invading fluorescently labeled HDFC matrix. Invadopodia are visualized as aggregates of colocalized actin and MT1-MMP penetrating deep into HDFC matrix. Arrowheads track individual invadopodia through consecutive z planes. Insets provide magnified views of invadopodia. (D) Representative Western blot of MT1-MMP knockdown with independent single duplex MT1-MMP-specific siRNA (si#1 and si#2). Control conditions: mock-transfected cells (not transfected [N/T]) and cells transfected with nonspecific control siRNA (N/S). (E) Representative morphologies of invadopodia of MDA-MB-231 cells invading HDFC. Arrows point to the filament-like extensions emanating from the actin/cortactin-rich cores of invadopodia. (F) H&E staining of intact or acellular normal breast tissue cryostat sections. (G) H&E staining of intact or acellular malignant breast tissue cryostat sections. (H) Immunostaining of MDA-MB-231 cells for actin and cortactin to identify actin/cortactin-rich invadopodia (yellow dots). Cells were allowed to invade into a 5% gelatin "cushion" for 3 h. Bars: [A–C [main images] and H] 10  $\mu$ m; (C, insets) 2  $\mu$ m; (E) 5  $\mu$ m; (F and G) 300  $\mu$ m.

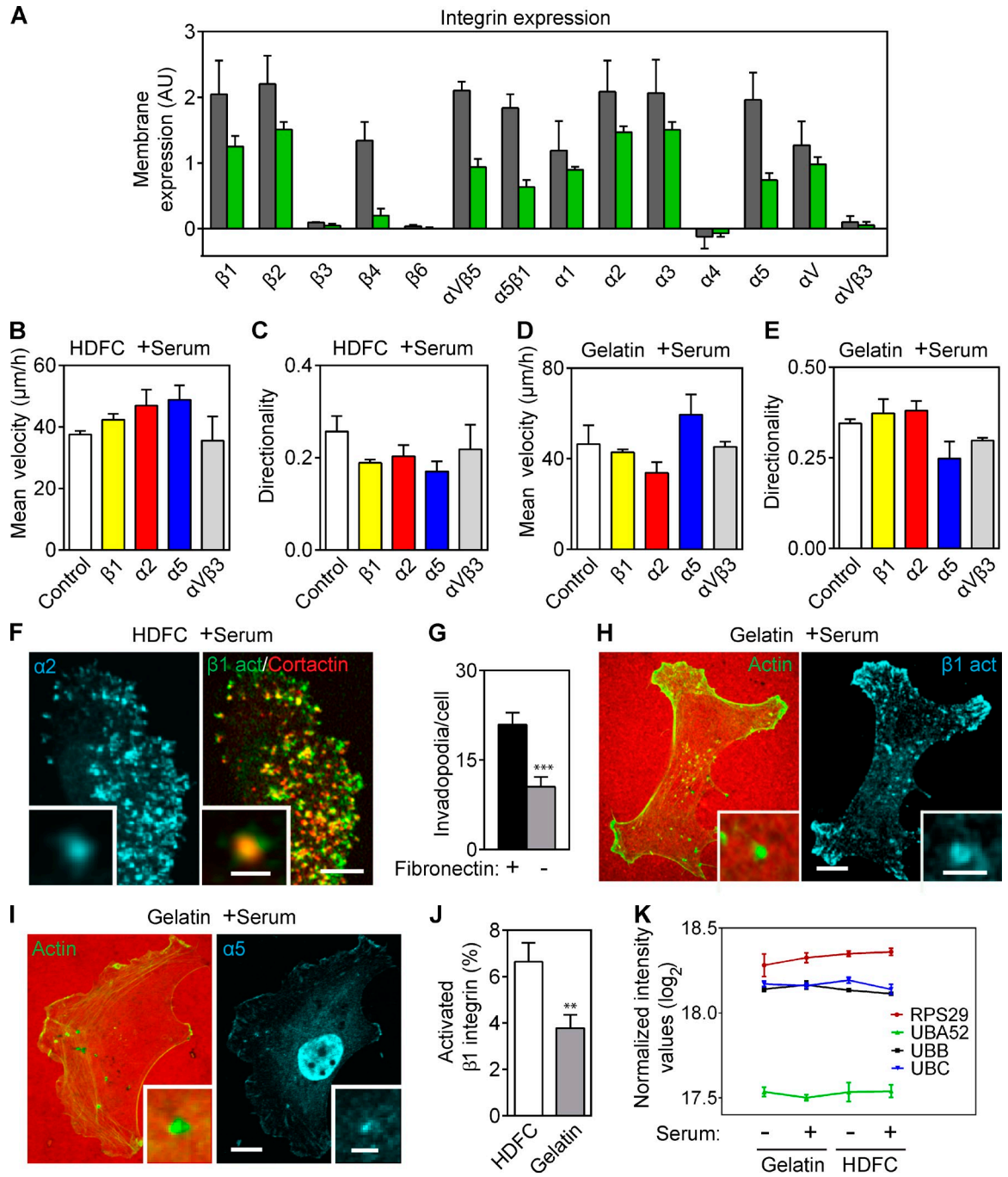
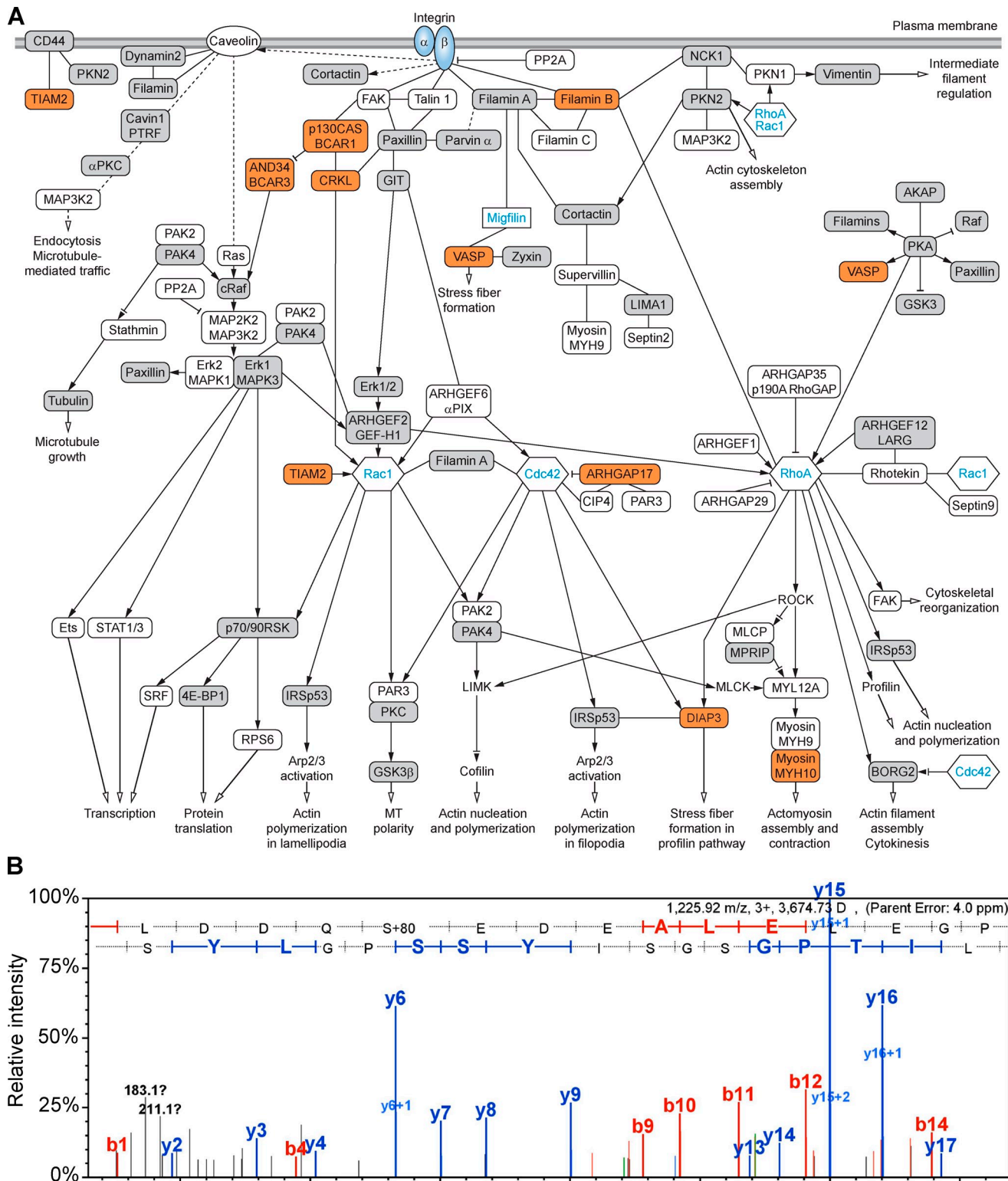


Figure S2. **Integrins and invadopodia formation.** (A) Cell surface integrin profiling of parental (gray) and wild-type c-Src-expressing (green) MDA-MD-231 cells as determined by  $\alpha$  and  $\beta$  integrin-mediated cell adhesion arrays (EMD Millipore). In these assays, microtiter plates precoated with mouse mAbs against individual human  $\alpha$  and  $\beta$  integrin subunits were used to capture cells expressing these integrins on their cell surface. Cells adhering to the microtiter plates were fixed and stained, and relative cell attachment was determined using absorbance spectrophotometry. Means  $\pm$  SEM from three independent experiments. AU, arbitrary unit. (B) Minimal effect of integrin inhibition on velocity of MDA-MB-231 carcinoma cells migrating on HDFC matrix in serum-containing media. The values are means  $\pm$  SEM of 30 cells from each of three independent experiments (i.e., a total of 90 cells for each condition). (C) Minimal effect of integrin inhibition on directionality of MDA-MB-231 carcinoma cells migrating on HDFC matrix in serum-containing media showing means  $\pm$  SEM of 30 cells from each of three independent experiments (total of 90 cells/condition). (D) Minimal effect of integrin inhibition on velocity of MDA-MB-231 cells migrating on gelatin matrix in serum-containing media. The values are means  $\pm$  SEM of 30 cells from each of three independent experiments. (E) Minimal effect of integrin inhibition on directionality of MDA-MB-231 cells migrating on gelatin matrix in serum-containing media. The values are means  $\pm$  SEM of 30 cells/condition, three independent repeats. (F) Immunolocalization of  $\alpha 2$  and activated  $\beta 1$  integrins ( $\beta 1$  act) to invadopodia of MDA-MB-231 cells invading HDFC. Insets show magnified individual invadopodia. (G) Effect of fibronectin depletion from serum on the invadopodia formation wild-type c-Src-overexpressing MDA-MB-231 cells. Full-length fibronectin was removed from the fetal bovine serum by passing it through gelatin-Sepharose column. Cells were incubated overnight on gelatin matrix in culture medium supplemented with fibronectin-depleted serum. Invadopodia were quantified as actin/cortactin aggregates. 19 cells were examined for each condition. The values are means  $\pm$  SEM. (H) Localization of activated  $\beta 1$  integrin to invadopodia of MDA-MB-231 cells invading gelatin matrix in serum-containing medium. Insets provide magnified views of invadopodia. (I) Localization of endogenous  $\alpha 5$  integrin to invadopodia of MDA-MB-231 cells invading gelatin. Insets show enlarged views of invadopodia. (J) Quantification of activated  $\beta 1$  integrin on cells adherent to HDFC or gelatin. The values indicate the percentage of the total ventral cell membrane positive for activated  $\beta 1$  integrin  $\pm$ SEM based on 20 cells/condition. (K) Expression of control genes (*RPS29*, *UBB*, *UBA52*, and *UBC*) for the microarray assays using Agilent 4  $\times$  44K Whole Human Genome microarray chips. Means  $\pm$  SEM value of normalized intensity from five independent experiments. \*\*,  $P < 0.001$ ; \*\*\*,  $P < 0.0001$ . Bars: (F, H, and I, main images) 10  $\mu\text{m}$ ; (F, H, and I, insets) 2  $\mu\text{m}$ .



**Figure S3. Phosphoproteomics analysis of cells adherent to gelatin matrix reveals complex downstream signaling network.** (A) White boxes indicate phosphoproteins identified in both HDFC and gelatin samples that have the same phosphorylation sites. Gray boxes denote phosphoproteins identified in both HDFC and gelatin samples that have different phosphorylation sites on the two different matrices. Orange boxes indicate phosphoproteins unique to gelatin matrix. Certain proteins without phosphorylation changes, including Rac1, Cdc42, RhoA,  $\alpha\beta$  integrin, and migfilin, have been inserted to clarify the signaling context of the proteins identified by phosphoproteomics. Solid lines indicate known direct physical binding between proteins. Dotted lines indicate indirect interactions involving intermediate partners. A black arrow at the end of a line indicates that a protein is known to stimulate the downstream signaling partner, lines with inhibition symbol indicate down-regulation of activity of the downstream signaling partner, lines with inhibition symbol plus a black arrow indicates both potential activation and inhibition, and open arrows denote stimulation of the cellular process. Abbreviations used in the signaling network diagram: VASP, vasodilator-stimulated phosphoprotein; CRKL, v-crk sarcoma virus CT10 oncogene homologue (avian)-like; GIT, G protein-coupled receptor kinase interacting ArfGAP 1; LARG, leukemia-associated Rho GEF. (B) MS/MS spectrum of the triply charged phosphopeptide, KLDGQSpEDEALELEGLITPGSGSIYSSPGLYSK, from kindlin2 at  $m/z = 1,225.92$  (bold indicates phosphorylated serine). The spectrum was obtained from the analysis of the phosphopeptide enriched tryptic digest derived from cells grown on HDFC matrix. Matched b- and y-ion fragments are highlighted in red and blue, respectively. Observation of the b9–12, 14, and 30 ions provides evidence for the localization of the phosphorylation on S159. The peptide was identified with a MASCOT identity score of 61.4. This phosphopeptide was not identified in samples derived from cells grown on a 2D gelatin matrix.

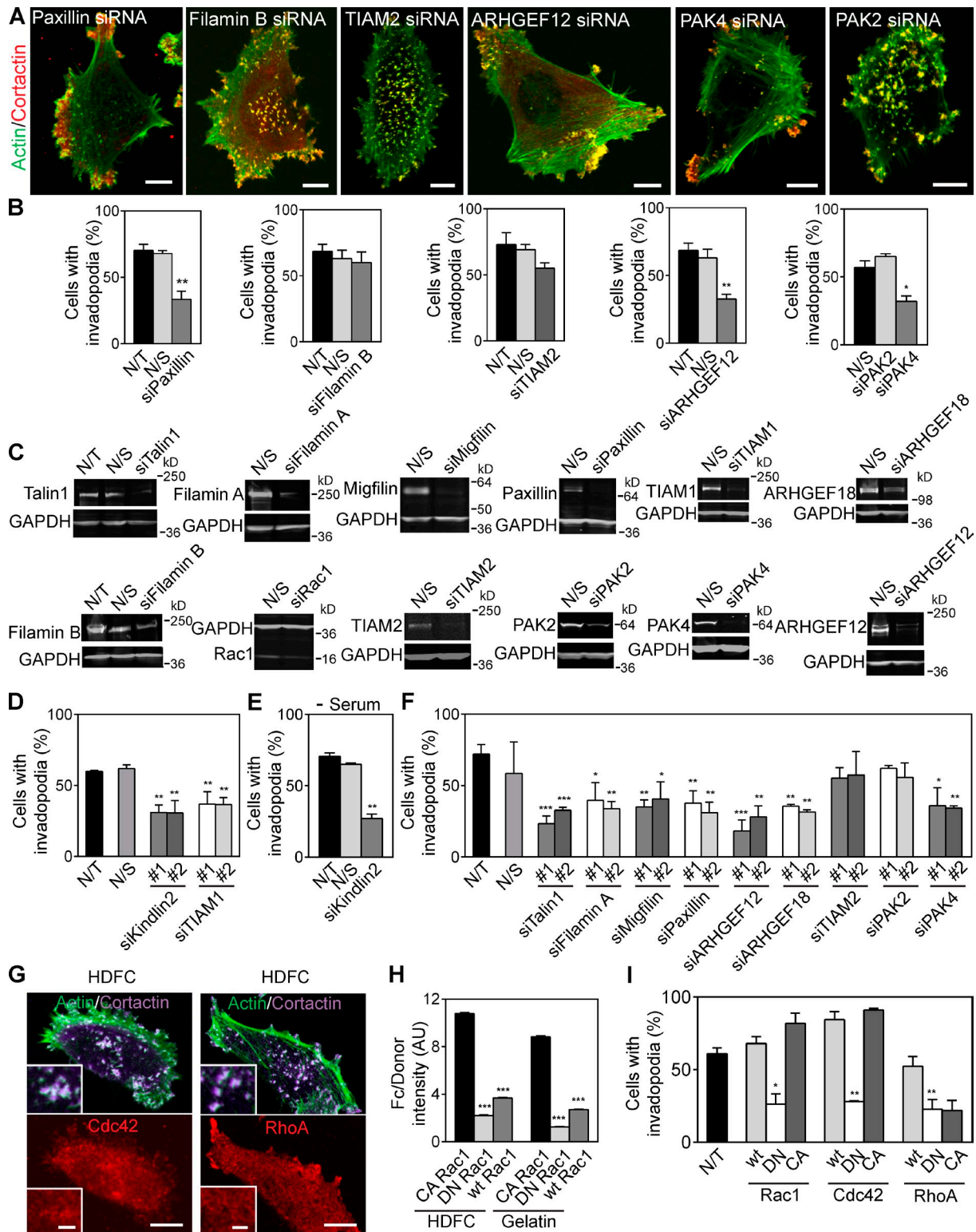
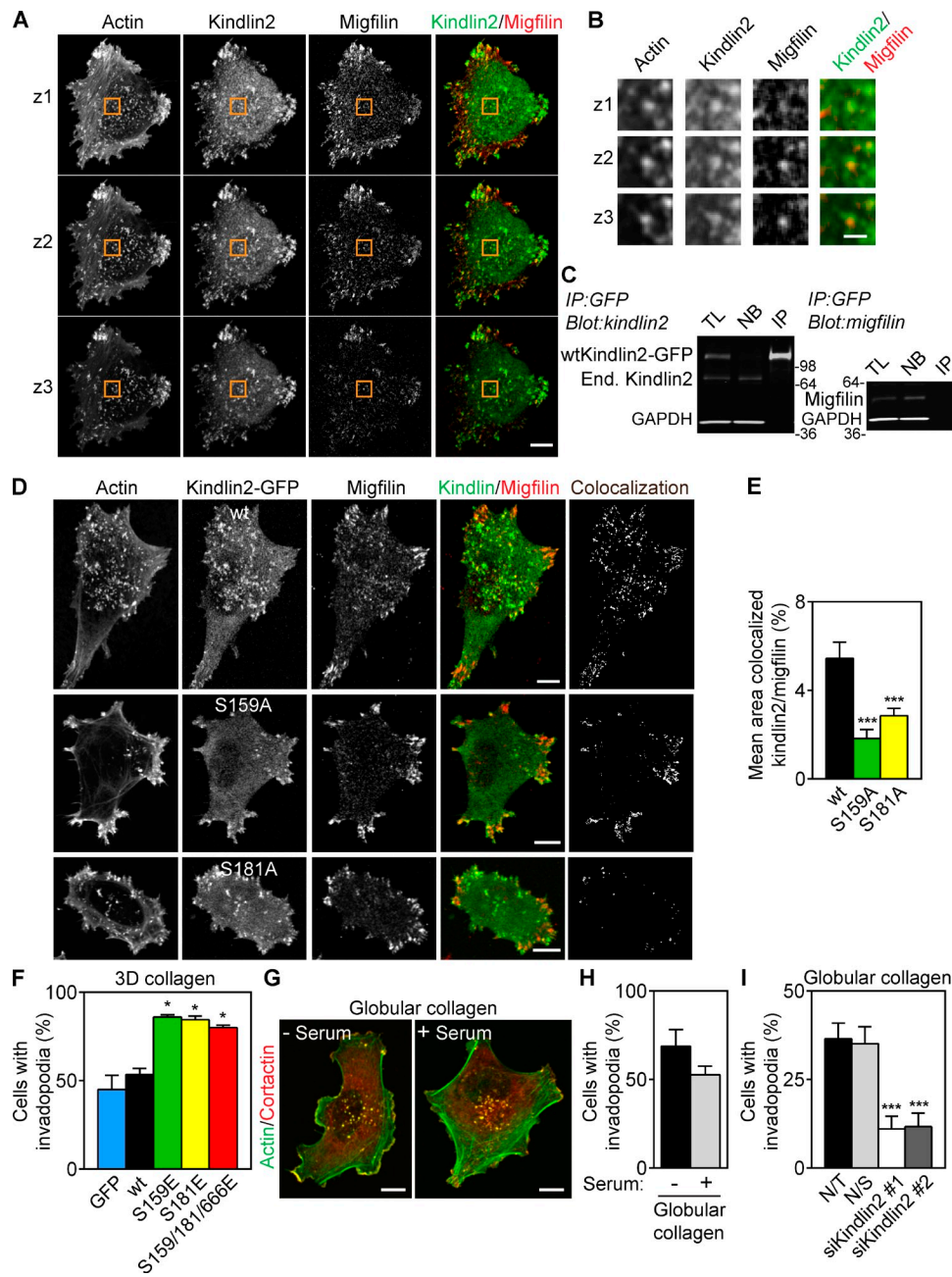


Figure S4. **Complex signaling network of multiple cellular proteins is required for invadopodia formation on HDFC.** (A) Representative immunofluorescence images of MDA-MB-231 cells invading HDFC after depletion of paxillin, filamin B, TIAM2, ARHGEF12, PAK4, or PAK2 using specific siRNA pools. (B) Quantitative evaluation of effects of specific protein knockdown in A on invadopodia formation in MDA-MB-231 cells. Means  $\pm$  SEM of  $\sim$ 100 cells from three independent experiments. (C) Representative Western blots for specific protein knockdown in A and B and in Fig. 5 (F–I, L, M, Q, and R). (D) Quantitative evaluation of protein knockdown on invadopodia formation in MDA-MB-231 cells using single duplex siRNA specific to kindlin2 and TIAM1. Values are means  $\pm$  SEM of  $\sim$ 100 cells/condition with three repeats. (E) Quantitative evaluation of kindlin2 down-regulation by siRNA pool on invadopodia formation on HDFC at the absence of serum. Values are means  $\pm$  SEM of  $\sim$ 100 cells/condition with two repeats. (F) Quantitative evaluation of protein knockdown on invadopodia formation in MDA-MB-231 cells using independent single duplex siRNAs specific to talin1, filamin A, migfilin, paxillin, ARHGEF12 and 18, TIAM2, PAK2, and PAK4. Values are means  $\pm$  SEM of  $\sim$ 100 cells/condition with three repeats. (G) Immunostaining of endogenous Cdc42 and RhoA in MDA-MB-231 cells invading HDFC. Insets show magnified views of invadopodia. (H) FRET efficiency of Rac1 biosensor for constitutively active (CA Rac1), dominant-negative (DN Rac1), and wild-type (wt Rac1) of the Rac1 biosensor. AU, arbitrary unit. (I) Effect of overexpression of wild-type (wt) small GTPases Rac1, Cdc42, RhoA, and their dominant-negative (DN) or constitutively active (CA) mutants on invadopodia formation in carcinoma cells invading HDFC. The values are mean percentages of cells with invadopodia  $\pm$  SEM of 100 cells/repeat with three independent repeats (300 cells total). N/S, nonspecific; N/T, nontransfected. \*,  $P < 0.05$ ; \*\*,  $P < 0.001$ ; \*\*\*,  $P < 0.0001$ . Bars: (A and G, main images) 10  $\mu$ m; (G, insets) 2  $\mu$ m.



**Figure S5. Kindlin2 phosphorylation regulates invadopodia formation in MDA-MB-231 cells on collagen matrices.** (A) Consecutive confocal z planes of the cell membrane adherent to HDFC matrix. Breast carcinoma MDA-MB-231 cells were cultured on HDFC matrix for 3 h, fixed, and immunolabeled for endogenous kindlin2, migfilin, and actin. Colocalization of kindlin2 and migfilin was detected as appearance of yellow color in kindlin2/migfilin overlay panel. (B) Magnified view of the boxed areas in A. (C) Representative Western blot of kindlin2 and migfilin coimmunoprecipitation (IP). Coimmunoprecipitation of exogenously expressed wild-type (wt) kindlin2-GFP and endogenous migfilin from cell lysates of MDA-MB-231 cells invading HDFC. The following protein fractions were loaded on the gels: TL, total cell lysate of MDA-MB-231 cells obtained from the cell lysis with RIPA lysis buffer; NB, not bound to immunoprecipitation beads fraction of the cell lysate; IP, immunoprecipitation fraction collected as eluent of the proteins bound to the immunoprecipitation beads. Blot on the left represents immunoprecipitation of GFP that was blotted for kindlin2 and GAPDH. Blot on the right represents IP of GFP blotted for migfilin and GAPDH. Molecular markers are in kilobases. Similar results for kindlin2-GFP and migfilin were obtained for other immunoprecipitation protocols listed in Materials and methods section and Western blot images were deposited to DataViewer database of JCB. (D) Confocal images of MDA-MB-231 cells expressing wild-type kindlin2-GFP or kindlin2-GFP mutants S159A or S181A. Cells overexpressing kindlin2-GFP constructs were incubated on HDFC for 3 h, fixed, and immunolabeled for endogenous migfilin and actin. Colocalization image is a binary (black and white) representation of a yellow color corresponding to colocalized kindlin2-GFP and migfilin in kindlin2-migfilin overlay images. (E) Quantification of colocalization of kindlin2-GFP and endogenous migfilin as measured by confocal microscopy in D. Data are the mean area of the kindlin2-GFP/migfilin colocalization normalized to the total area of the cell  $\pm$  SEM from 10–20 cells/condition. (F) Effect of expression of kindlin2 phosphomimetic mutants on invadopodia formation in MDA-MB-231 cells invading thin 3D collagen matrix polymerized at 1.3 mg/ml concentration. Cells were cultured on 3D collagen in the absence of serum. Means  $\pm$  SEM of  $\sim$ 100 cells/condition with two repeats. (G) Representative images of MDA-MB-231 carcinoma cells cultured on globular collagen in the absence or presence of serum. Invadopodia are visualized as yellow aggregates of colocalized actin and cortactin. (H) Quantification of invadopodia-positive cells in G. The values are mean percent of cells with invadopodia  $\pm$  SEM of 90–100 cells/repeat with two to three independent repeats. (I) Quantitative evaluation of the effects of protein knockdown on invadopodia formation in MDA-MB-231 cells using independent single duplex siRNAs specific to kindlin2. Controls are mock transfection (not transfected [N/T]) and cell transfection with nonspecific single duplex siRNA (N/S). The effect of kindlin2 depletion was assayed on cells invading globular collagen matrix. Values are means  $\pm$  SEM of  $\sim$ 100 cells/condition with three repeats. \*,  $P < 0.05$ ; \*\*\*,  $P < 0.0001$ . Bars: (A, D, and G) 10  $\mu$ m; (B) 2  $\mu$ m.

Table S1. **Integrin signaling network phosphoproteins and their phosphosites**

Symbol	Entrez gene name	UniProt/Swiss 2D gelatin	2D gelatin phosphosites	UniProt/Swiss HDFC	HDFC phosphosites
4EBP1	Eukaryotic translation initiation factor 4E binding protein 1	4EBP1_HUMAN	Y34, T37, T41, S44, T45, T46, T50, S65, T68, T70	4EBP1_HUMAN	Y34, S35, T36, T37, T41, S44, T45, T46, T50, S65, T68, T70, T77, T82
AKAP	A kinase (PRKA) anchor protein 11	AKA11_HUMAN	S1170, S1172	AKA11_HUMAN	S1170, S1172, T1174
AKAP	A kinase (PRKA) anchor protein 2	AKAP2_HUMAN	S121, S152, S154, S155, S158, S393, T399, S748	AKAP2_HUMAN	S152, S154, S159, S393, T399, S748
ARHGAP17	Rho GTPase-activating protein 17	RHG17_HUMAN	T679	–	–
ARHGAP29	Rho GTPase-activating protein 29	RHG29_HUMAN	S930, S1029	RHG29_HUMAN	S930, S1029
ARHGAP35	Rho GTPase-activating protein 35, p190A RhoGAP	RHG35_HUMAN	S1179	RHG35_HUMAN	S1179
ARHGAP5	Rho GTPase-activating protein 5, p190B RhoGAP	–	–	RHG05_HUMAN	S1195
ARHGEF1	Rho GEF 1	ARHG1_HUMAN	S863	ARHG1_HUMAN	S863
ARHGEF12	Rho GEF 12	ARHGC_HUMAN	S341, T736	ARHGC_HUMAN	T736
ARHGEF18	Rho/Rac GEF 18	–	–	ARHG1_HUMAN	S1103
ARHGEF2	Rho/Rac GEF 2; GEF-H1	ARHG2_HUMAN	S151, T152, T153, S174, T175, T695, S696, S886	ARHG2_HUMAN	S149, S151, T152, S174, T695, S696, S886
ARHGEF6	Rac/Cdc42 GEF 6, $\alpha$ PIX	ARHG6_HUMAN	S488	ARHG6_HUMAN	S488
BCAR1	breast cancer anti-estrogen resistance 1, p130CAS	BCAR1_HUMAN	Y362	–	–
BCAR3	breast cancer anti-estrogen resistance 3, AND34	BCAR3_HUMAN	S363	–	–
BORG2	CDC42 effector protein (Rho GTPase binding) 3	BORG2_HUMAN	S89, S108, T111, S115	BORG2_HUMAN	S100, S108, S115
Caveolin	caveolin 1, caveolae protein, 22 kD	CAV1_HUMAN	S37	CAV1_HUMAN	S37
Cavin1/PTRF	Polymerase I and transcript release factor (PTRF)	PTRF_HUMAN	S169, T302	PTRF_HUMAN	S169, S300, T302
CD44	CD44 molecule (Indian blood group)	CD44_HUMAN	S704, S706	CD44_HUMAN	S706
CIP4	Cdc42-interacting protein 4	CIP4_HUMAN	S296	CIP4_HUMAN	S296
Cortactin	cortactin	SRC8_HUMAN	T401, S405, T411, S417, S418, Y421	SRC8_HUMAN	T399, T401, S405, T411, S418, Y421
CRKL	v-crk sarcoma virus CT10 oncogene homologue (avian)-like	CRKL_HUMAN	Y207, S222	–	–
DIAP3	diaphanous homologue 3 ( <i>Drosophila melanogaster</i> )	DIAP3_HUMAN	S1093	–	–
Dynamin2	dynamin 2	DYN2_HUMAN	T755, S764	DYN2_HUMAN	T743, S759
Ets	v-ets erythroblastosis virus E26 oncogene homologue 1 (avian)	ETS1_HUMAN	S282	ETS1_HUMAN	S282
FAK	PTK2 protein tyrosine kinase 2	FAK1_HUMAN	S910	FAK1_HUMAN	S910
Filamin A	filamin A, $\alpha$	FLNA_HUMAN	S1084, S1459	FLNA_HUMAN	S1084, S1454, S1459
Filamin B	filamin B, $\beta$	FLNB_HUMAN	S2478	–	–
Filamin C	filamin C, $\gamma$	FLNC_HUMAN	S2233	FLNC_HUMAN	S2233
GIT	G protein-coupled receptor kinase interacting ArfGAP 1	GIT1_HUMAN	S362	GIT1_HUMAN	S362, S592
GSK3 $\beta$	glycogen synthase kinase 3 $\beta$	GSK3B_HUMAN	T8, S9, Y216	GSK3B_HUMAN	S9, Y216
IRSp53	BAI1-associated protein 2	BAIP2_HUMAN	S338, T340	BAIP2_HUMAN	T340, T455
Kindlin2	fermitin family member 2	–	–	FERM2_HUMAN	S159
LIMA1	LIM domain and actin binding protein	LIMA1_HUMAN	S362, S365, S490	LIMA1_HUMAN	S362, S373, T487, S490, S604
MAP2K2	mitogen-activated protein kinase kinase 2, MEK2	MP2K2_HUMAN	S222, S226, T394, T396	MP2K2_HUMAN	S222, S226, T394, T396
MAP3K2	mitogen-activated protein kinase kinase kinase 2, MEK1	M3K2_HUMAN	S164	M3K2_HUMAN	S164
MAPK1	mitogen-activated protein kinase 1, Erk2	MK01_HUMAN	T185, Y187	MK01_HUMAN	T185, Y187
MAPK3	mitogen-activated protein kinase 3, Erk1	MK03_HUMAN	T202, Y204	MK03_HUMAN	T202

Table S1. **Integrin signaling network phosphoproteins and their phosphosites** (Continued)

Symbol	Entrez gene name	UniProt/Swiss 2D gelatin	2D gelatin phosphosites	UniProt/Swiss HDFC	HDFC phosphosites
MLCP	protein phosphatase 1, regulatory subunit 10; PPP1R10	PP1RA_HUMAN	S313	PP1RA_HUMAN	S313
MLCP	protein phosphatase 1, regulatory subunit 12A; PPP1R12A; myosin phosphatase target subunit 1	MYPT1_HUMAN	S422, T443, S445, Y446	MYPT1_HUMAN	S299, S422, T443, S445, Y446, S862
MLCP	protein phosphatase 1, regulatory (inhibitor) subunit 14B; PPP1R14B	PP14B_HUMAN	S32	PP14B_HUMAN	S32
MPRIP	myosin phosphatase Rho interacting protein	MPRIP_HUMAN	S619, S977, S980, S993	MPRIP_HUMAN	S540, S619, S977, S993
MYL12A	myosin, light chain 12A, regulatory, nonsarcomeric	ML12A_HUMAN	T18, S19	ML12A_HUMAN	T18, S19
Myosin MYH10	myosin, heavy chain 10, nonmuscle	MYH10_HUMAN	S1956	–	
Myosin MYH9	myosin, heavy chain 9, nonmuscle	MYH9_HUMAN	S1943	MYH9_HUMAN	S1943
NCK1	noncatalytic region of tyrosine kinase (NCK) adaptor protein 1	NCK1_HUMAN	S85	NCK1_HUMAN	S85, S91
NF-κB	nuclear factor of κ light polypeptide gene enhancer in B-cells 1	–		NFKB1_HUMAN	S907
p70RSK	ribosomal protein S6 kinase, 70 kD, polypeptide 1	KS6B1_BOVIN	S447	KS6B1_BOVIN	S447
p90RSK	ribosomal protein S6 kinase, 90 kD, polypeptide 3	KS6A3_HUMAN	S227, T231	KS6A3_HUMAN	S227, T231, T577
p90RSK	ribosomal protein S6 kinase, 90 kD, polypeptide 4	KS6A4_HUMAN	S682, T687	KS6A4_HUMAN	S347, S682, T687
PAK2	p21 protein (Cdc42/Rac)-activated kinase 2	PAK2_HUMAN	S141, T143	PAK2_HUMAN	S141, T143
PAK4	p21 protein (Cdc42/Rac)-activated kinase 4	PAK4_HUMAN	S104, S181, T207, S474	PAK4_HUMAN	S181, T207, S474, T478
PAR3	par-3 partitioning defective 3 homologue ( <i>Caenorhabditis elegans</i> )	PARD3_HUMAN	S144	PARD3_HUMAN	S144
Parvin α	parvin, α	PARVA_HUMAN	S14, S19	PARVA_HUMAN	S10, S14, S19
Paxillin	paxillin	PAXI_HUMAN	S84, S85, S106, S303, S322	PAXI_HUMAN	S84, S85, S106, S244, S303, S322
PKA	protein kinase, cAMP-dependent, catalytic, β	KAPCB_HUMAN	T196, T198, T202	KAPCB_HUMAN	T196, T198
PKA	protein kinase, AMP-activated, γ 2 noncatalytic subunit	AAKG2_HUMAN	S83, S196	AAKG2_HUMAN	S196
PKA	protein kinase, cAMP-dependent, regulatory, type I, α (tissue-specific extinguisher 1)	KAPO_HUMAN	S87, S93	KAPO_HUMAN	S87, S93
PKA	protein kinase, cAMP-dependent, regulatory, type II, α	KAP2_HUMAN	S109	KAP2_HUMAN	S109
PKC	protein kinase C, α	KPCA_HUMAN	T495, T497, T501	KPCA_HUMAN	S226, T497, T501
PKC	protein kinase C, δ	KPCD_HUMAN	S506, T507	KPCD_HUMAN	S506, T507
PKC	protein kinase C, ι	KPCI_HUMAN	T409, S411, T412, T564	KPCI_HUMAN	S411, T412, T564
PKN1	protein kinase N1	PKN1_HUMAN	S773, T774, T778	PKN1_HUMAN	S773, T774, T778
PKN2	protein kinase N2	PKN2_HUMAN	S815, T816, T820, T958	PKN2_HUMAN	T814, S815, T816, T820, T958
PP2A	protein phosphatase 2, regulatory subunit B', δ	2A5D_HUMAN	S573	2A5D_HUMAN	S573
Raf	v-raf-1 murine leukemia viral oncogene homologue 1	RAF1_HUMAN	T258, S259, T260	RAF1_HUMAN	S257, T258, S259, T260, S642
Ras	related RAS viral (r-ras) oncogene homologue 2	RRAS2_HUMAN	S186	RRAS2_HUMAN	S186
Rhotekin	rhotekin	RTKN_HUMAN	S520	RTKN_HUMAN	S520
RPS6	ribosomal protein S6	RS6_HUMAN	S236	RS6_HUMAN	S236
Septin2	septin 2	SEPT2_HUMAN	S218	SEPT2_HUMAN	S218
Septin9	septin 9	SEPT9_HUMAN	S30	SEPT9_HUMAN	S30
SRF	serum response factor (c-fos serum response element-binding transcription factor)	SRF_HUMAN	S224	SRF_HUMAN	S224

Table S1. **Integrin signaling network phosphoproteins and their phosphosites** (Continued)

Symbol	Entrez gene name	UniProt/Swiss 2D gelatin	2D gelatin phosphosites	UniProt/Swiss HDFC	HDFC phosphosites
STAT1	signal transducer and activator of transcription 1, 91 kD	STAT1_HUMAN	S727	STAT1_HUMAN	S727
STAT3	signal transducer and activator of transcription 3 (acute-phase response factor)	STAT3_BOVIN	S727	STAT3_BOVIN	S727
Stathmin	stathmin 1	STMN1_HUMAN	S16, S25, S38	STMN1_HUMAN	S16, S25, S38
Supervillin	Supervillin	SVIL_HUMAN	S245, T852	SVIL_HUMAN	S245, T852
Talin1	talín 1	TLN1_HUMAN	S425	TLN1_HUMAN	S425
TIAM1	T-cell lymphoma invasion and metastasis 1	–	–	TIAM1_HUMAN	S231
TIAM2	T-cell lymphoma invasion and metastasis 2	TIAM2_HUMAN	S720	–	–
Tubulin	tubulin, $\alpha$ 1c	TBA1C_HUMAN	S488	TBA1C_HUMAN	S48, T51
VASP	vasodilator-stimulated phosphoprotein	VASP_HUMAN	S322, S323, S325, T328, T331	–	–
Vimentin	vimentin	VIME_HUMAN	T20, S39, S51, Y53, S55, S56, Y61, S73, S409, S412, S419, S420	VIME_HUMAN	S39, S42, Y53, S55, S56, S72, S73, S412, S419, S420, T426, S430
Zyxin	zyxin	ZYX_HUMAN	S143, S281, S308, S344	ZYX_HUMAN	S142, S143, S308, S344

Minus signs indicate that no phosphopeptides were detected for the protein.

Table S2. **List of +1 and +2 predicted fragment ions for the kindlin2 phosphopeptide KLDDQSpEDEALELEGLITPGSGSIYS SPGLYSK**

b	b ions	b +2H	b –NH <sub>3</sub>	b –H <sub>2</sub> O	AA	y ions	y +2H	y –NH <sub>3</sub>	y –H <sub>2</sub> O	y
1	129.1 <sup>a</sup>	65.1	112.1		K	3,675.7	1,838.4	3,658.7	3,657.7	34
2	242.2	121.6	225.2		L	3,547.6	1,774.3	3,530.6	3,529.6	33
3	357.2	179.1	340.2	339.2	D	3,434.5	1,717.8	3,417.5	3,416.5	32
4	472.2 <sup>a</sup>	236.6	455.2	454.2	D	3,319.5	1,660.3	3,302.5	3,301.5	31
5	600.3	300.7	583.3	582.3	Q	3,204.5	1,602.7	3,187.5	3,186.5	30
6	767.3	384.2	750.3	749.3	S + 80 <sup>b</sup>	3,076.4	1,538.7	3,059.4	3,058.4	29
7	896.3	448.7	879.3	878.3	E	2,909.4	1,455.2	2,892.4	2,891.4	28
8	1,011.4	506.2	994.3	993.4	D	2,780.4	1,390.7	2,763.4	2,762.4	27
9	1,140.4 <sup>a</sup>	570.7	1,123.4	1,122.4	E	2,665.4	1,333.2	2,648.3	2,647.4	26
10	1,211.4 <sup>a</sup>	606.2	1,194.4	1,193.4	A	2,536.3	1,268.7	2,519.3	2,518.3	25
11	1,324.5 <sup>a</sup>	662.8	1,307.5	1,306.5	L	2,465.3	1,233.1	2,448.3	2,447.3	24
12	1,453.6 <sup>a</sup>	727.3	1,436.5	1,435.6	E	2,352.2	1,176.6	2,335.2	2,334.2	23
13	1,566.7	783.8	1,549.6	1,548.6	L	2,223.2	1,112.1	2,206.1	2,205.1	22
14	1,695.7 <sup>a</sup>	848.4	1,678.7	1,677.7	E	2,110.1	1,055.5	2,093.0	2,092.1	21
15	1,752.7	876.9	1,735.7	1,734.7	G	1,981.0	991.0	1,964.0	1,963.0	20
16	1,849.8	925.4	1,832.7	1,831.8	P	1,924.0	962.0	1,907.0	1,906.0	19
17	1,962.9	981.9	1,945.8	1,944.8	L	1,827.0	914.0	1,809.9	1,808.9	18
18	2,075.9	1,038.5	2,058.9	2,057.9	I	1,713.9 <sup>c</sup>	857.4	1,696.8	1,695.9	17
19	2,177.0	1,089.0	2,160.0	2,159.0	T	1,600.8 <sup>c</sup>	800.9	1,583.8	1,582.8	16
20	2,274.0	1,137.5	2,257.0	2,256.0	P	1,499.7 <sup>c</sup>	750.4 <sup>c</sup>	1,482.7	1,481.7	15
21	2,331.1	1,166.0	2,314.0	2,313.1	G	1,402.7 <sup>c</sup>	701.8	1,385.7	1,384.7	14
22	2,418.1	1,209.6	2,401.1	2,400.1	S	1,345.7 <sup>c</sup>	673.3	1,328.6	1,327.7	13
23	2,475.1	1,238.1	2,458.1	2,457.1	G	1,258.6	629.8	1,241.6	1,240.6	12
24	2,562.1	1,281.6	2,545.1	2,544.1	S	1,201.6 <sup>c</sup>	601.3	1,184.6	1,183.6	11
25	2,675.2	1,338.1	2,658.2	2,657.2	I	1,114.6	557.8	1,097.6	1,096.6	10
26	2,838.3	1,419.7	2,821.3	2,820.3	Y	1,001.5 <sup>c</sup>	501.3	984.5	983.5	9
27	2,925.3	1,463.2	2,908.3	2,907.3	S	838.4 <sup>c</sup>	419.7	821.4	820.4	8
28	3,012.4	1,506.7	2,995.3	2,994.4	S	751.4 <sup>c</sup>	376.2	734.4	733.4	7
29	3,109.4	1,555.2	3,092.4	3,091.4	P	664.4 <sup>c</sup>	332.7	647.3	646.4	6
30	3,166.4	1,583.7 <sup>a</sup>	3,149.4	3,148.4	G	567.3	284.2	550.3	549.3	5
31	3,279.5	1,640.3	3,262.5	3,261.5	L	510.3 <sup>c</sup>	255.6	493.3	492.3	4
32	3,442.6	1,721.8	3,425.6	3,424.6	Y	397.2 <sup>c</sup>	199.1	380.2	379.2	3
33	3,529.6	1,765.3	3,512.6	3,511.6	S	234.1 <sup>c</sup>	117.6	217.1	216.1	2
34	3,675.7	1,838.4	3,658.7	3,657.7	K	147.1	74.1	130.1		1

Table S3. **List of siRNA sequences used in this paper**

siRNA name	Type	siRNA sequence
Kindlin2	Pool	AAUGAAAUCUGGCUUCGUU; GAACUGAGUGUCAUGUGA; CUACAUUUUCUCUCAACA; GCCCAGGACUGUAUAGUAA
Kindlin2	Single duplexes	AAUGAAAUCUGGCUUCGUU; CUACAUUUUCUCUCAACA
Talin 1	Pool	GAAGAUGGUUGGCGGCAUU; GUAGAGGACCUGACAACAA; UCAAUCAGCUCAUCACUAI; GAGAUGAGGAGUCUACUAI
Talin1	Single duplexes	GAAGAUGGUUGGCGGCAUU; GUAGAGGACCUGACAACAA
Filamin A	Pool	GCAGGAGGCUUGGCGAGUAI; GCACCCAGACCGUCAAUUA; GCACAUGUUCGGUGUCCUA; GAAUGGCGUUUACCGUAU
Filamin A	Single duplexes	GCACAUGUUCGGUGUCCUA; GAAUGGCGUUUACCGUAU
Filamin B	Pool	GCGAUGCAGUGAAGGAUUU; GCACGGUCACUGUUAGAU; CAAGGUAGCCAUCCUCAGA; UACAUUCG AUGACCAUAAA
Migfilin	Pool	GAAGAGGGUGGCAUCGUCU; GCAUUGGGGAUGAGAGCUU; CCAUGAAGAGGCAGUACCA; UGUACUGCCUGGACGACU
Migfilin	Single duplexes	CCAUGAAGAGGCAGUACCA; UGUACUGCCUGGACGACU
TIAM1	Pool	CAAAUJAGCCAUAGCAACA; GAACCGAAGCUGUAAAAGAA; GUAUAAAAGAUUGGUCCAAA; GCAGGCUACUGUCGGAAU
TIAM1	Single duplexes	CAAAUJAGCCAUAGCAACA; GCAGGCUACUGUCGGAAU
TIAM2	Pool	GUGUAAGGAUCGCCUGGUA; GAGCACUUCUCCCGGGAAA; CGACCUAAAUCUGUUCUA; GAACUUCAGGCGUCACAU
TIAM2	Single duplexes	GAGCACUUCUCCCGGGAAA; GUGUAAGGAUCGCCUGGUA
ARHGEF12	Pool	GAUCAAAUCUCGUCAGAAA; GAAUGAGACCUCUGUUAI; GGACAUUGCCUUUAGAA; GGCAACAUUUCCAAAGUA
ARHGEF12	Single duplexes	GAUCAAAUCUCGUCAGAAA; GAAUGAGACCUCUGUUAI
ARHGEF18	Pool	GGACGCAACUCGGACCAAU; CACAACGCAUAACCAAAUA; GCAGUGACCGGAAUUAUGU; UCAGGGCGCUUGAAAAGUA
ARHGEF18	Single duplexes	GGACGCAACUCGGACCAAU; UCAGGGCGCUUGAAAAGUA
Paxillin	Pool	CAACUGGAAACCACACAUAI; GGACGUGGCACCCUGAACAU; CCAAACGGCCUGUGUUCUUU; UGACGAAAAGAGAAGCCUAI
Paxillin	Single duplexes	CAACUGGAAACCACACAUAI; UGACGAAAAGAGAAGCCUAI
Rac1	Pool	GUGAUUUCAUAGCGAGUUU; GUAGUUCUCAGAUGCUGUA; AUGAAAUGUGUCACGGGUAA; GAACUGCUAUUUCUCUA
PAK2	Pool	GAACUGAUCAUUACGAGA; ACAGUGGGCUCGAUUACUA; GAGCAGAGCAAACGCAGUA; GAAACUGGCCAAACCGUUA
PAK2	Single duplexes	GAAACUGGCCAAACCGUUA; GAGCAGAGCAAACGCAGUA
PAK4	Pool	GAGUAUCCAUAGAGCAGUU; GGAUAAUGGUGAUUGAGAU; CCAUGAAGAUGAUUCGGGA; GGGACUACCAGCACGAGAA
PAK4	Single duplexes	CCAUGAAGAUGAUUCGGGA; GGGACUACCAGCACGAGAA
N/S control	Pool	ON-TARGET plus control nontargeting siRNA/Thermo Fisher Scientific catalog number D-001810-10
N/S control	Single duplexes	ON-TARGET plus control nontargeting siRNA/Thermo Fisher Scientific catalog number D-001810-01

All sequences in the table are shown starting with 5' and ending with 3' ends. N/S, nonspecific.

Table S4. **List of primers used for constructing human kindlin2 cDNA.**

Vector type	Forward primer	Reverse primer
GFP	GGATCCAGGAATGGTGAAGGCGGAGGAGCTG	GAACTTGC GGCCGCTTACTTGTACAGCTCGTC
WT	GCTAGCGGCCACCATGGCTCTGGACGGGATAAGGATGCCA	GGATCCCCTGAGTTACCCACCAACCACTGGTAAGTTTG
S159A	AAGAAGCTAGATGACCAGGCTGAAGATGAGGCACCTGAATTA	TAATTC AAGTGCCTCATCTTCAGCCTGGTCATCTAGCTTCTT
S181A	GGATCAGGAAGTATATATTCAGCGCCAGGACTGTATAGTAAAACA	TGTTTTACTATACAGTCCTGGCGCTGAATATATACTTCTGATCC
S666A	CGTGCAAAAGACCAAAACGAGGCATTAGATGAAGAGATGTTCTAC	GTAGAACATCTTTCATCTAATGCCTCGTTTTGGCTTTTGCACG
S159E	AAGAAGCTAGATGACCAGGAGGAAGATGAGGCACCTGAATTA	TAATTC AAGTGCCTCATCTTCTCCTGGTCATCTAGCTTCTT
S181E	GGATCAGGAAGTATATATTCAGAGCCAGGACTGTATAGTAAAACA	TGTTTTACTATACAGTCCTGGCTCTGAATATATACTTCTGATCC
S666E	CGTGCAAAAGACCAAAACGAGGAATTAGATGAAGAGATGTTCTAC	GTAGAACATCTTTCATCTAATTCCTCGTTTTGGCTTTTGCACG
siRNA rescue	GTTGCAGAAAGCATGAACGAGATTGGCTACGATGTGACAATGAA AAACAG	CTGTTTTTCATTGTACATCGTAGCCAAATCTCGTTTCATGCCTTCT GCAAC

All sequences in the table are shown starting with 5' and ending with 3' ends.

**A ZIP file is provided that includes a Matlab code for extracting elastic modulus from indentation data; the code uses nonlinear least squares fit with the coordinates of the contact point and the elastic modulus as the fitting parameters.**

**Dataset 1 is provided as an Excel file with AFM data corresponding to Table 1.**